

## Supplementary Information for

### Transformation of Carbon-Supported Pt-Ni Octahedral Electrocatalysts into Cubes: Toward Stable Electrocatalysis

Meital Shviro<sup>a†\*</sup>, Martin Gocyla<sup>a†</sup>, Roland Schierholz<sup>b</sup>, Hermann Tempel<sup>b</sup>, Hans Kungl<sup>b</sup>, Rüdiger A. Eichel<sup>b</sup> and Rafal E. Dunin-Borkowski<sup>a</sup>.

<sup>a</sup> Ernst Ruska-Centre for Microscopy and Spectroscopy with Electrons, Forschungszentrum Jülich GmbH, 52425 Jülich, Germany.

<sup>b</sup> Institute of Energy and Climate Research 9, Fundamental Electrochemistry, Forschungszentrum Jülich GmbH, 52425 Jülich, Germany.

The Supplementary Information includes:

- Experimental information and Figure S 1, Figure S 2, Figure S 3, Figure S 4, Figure S 5, Figure S 6, Figure S 7, Figure S 8, Figure S 9 and Figure S 10 – with additional TEM, STEM and EDX data.

## Experimental section

**Materials.** Aniline (99.5 %), tungsten hexacarbonyl ( $\text{W}(\text{CO})_6$ , 97.0 %), oleic acid (OAc, 90 %), oleylamine (OAm, 98.0 %) Benzyl alcohol (BA) and benzoic acid (99.5 % ACS) were purchased from sigma Aldrich. Platinum(II)acetylacetonate ( $\text{Pt}(\text{acac})_2$  (Pt 48 % min), Nickel(II)acetylacetonate ( $\text{Ni}(\text{acac})_2$ , 95 %), Toluene (99 %), Polyvinylpyrrolidone (PVP, MW=8000), 1-hexadecyltrimethyl ammonium bromide ( $\text{CH}_3(\text{CH}_2)_{15}\text{N}(\text{CH}_3)_3\text{Br}$ , CTAB, 98 %) was purchased from Alfa Aeser. Ethanol (96 % min,) was purchased from eal and carbon black (C, VXC72R) was purchased from CABOT. Acetone (technical grade) was purchased from VWR chemicals. All materials were used as received.

**Synthesis of Pt-Ni/C octahedral nanoparticles.** Octahedral Pt-Ni/C catalyst nanoparticles (NPs) were prepared by the simultaneous reduction of  $\text{Pt}(\text{acac})_2$  (0.025 mmol) and  $\text{Ni}(\text{acac})_2$  (0.02 mmol) using BA (10 ml) as both a solvent and a reducing agent. CTAB (0.047 mmol) and benzoic acid (0.49 mmol) were used as structure-directing agents. In a typical synthesis of octahedral Pt-Ni/C catalysts,  $\text{Pt}(\text{acac})_2$ ,  $\text{Ni}(\text{acac})_2$ , benzoic acid, CTAB, and C (0.008 g) were dispersed in BA. The mixture was then ultrasonicated for 10 min. The resulting homogeneous mixture was heated to 150 °C for 12 h in an oil bath, before being cooled naturally to room temperature. The resulting colloidal products were collected by centrifugation and washed several times with ethanol.

**Synthesis for irregular Pt-Ni/C reference nanoparticles.** Pt-Ni/C nanoparticles were synthesized using a route based on previous work<sup>1</sup>.  $\text{Pt}(\text{acac})_2$  (0.407 mmol),  $\text{Ni}(\text{acac})_2$  (0.934 mmol), OAm (48 mL) and OAc (32 mL) were added into a 100 ml three-neck-flask under reflux. The reaction mixture was stirred for 5 minutes under  $\text{N}_2$  atmosphere at 60 °C, followed by raising the temperature to 130 °C. At this temperature  $\text{W}(\text{CO})_6$  (1.59 mmol) was added rapidly,  $\text{N}_2$  purging was stopped and the reaction mixture was heated to 230 °C and then stirred for 50 min before the reaction mixture being cooled to room temperature and toluene (20 mL) and ethanol (60 mL) were added to the reaction mixture. The supernatant was removed by centrifugation (7800 rpm for 15 min) and dispersed in toluene (20 mL). The dispersion was added to a dispersion of C (160 mg) in toluene (20 mL). The mixture was sonicated with an ultrasonic horn for 30 min. Afterwards ethanol (10 mL) was added and the catalyst was centrifuged (7800 rpm for 15 min) and washed with ethanol (30 mL) three times.

**Synthesis for Pt-Ni reference nanoparticles without C.** Pt-Ni nanoparticles were synthesized using a route based on previous work<sup>2</sup>.  $\text{Pt}(\text{acac})_2$  (0.2 mmol),  $\text{Ni}(\text{acac})_2$  (0.93 mmol), PVP (0.8 g) and aniline (5 ml) were dissolved in 50 ml of BA with 30 min vigorous stirring and transferred into a 100 ml Ace pressure gas flask. The flask was heated to 150 °C for 12 h before being cooled naturally to room

temperature. Pt-Ni nanoparticles were precipitated by acetone, separated *via* centrifugation, and purified by an ethanol-acetone mixture.

***In situ* transmission electron microscopy (TEM) measurements under reducing conditions.** The C-supported Pt-Ni octahedral nanoparticles were dispersed on a MEMS chip (DENSsolutions B.V.), which was loaded into a DENSsolutions TEM heating holder for *in situ* thermal annealing studies.

**Core-shell octahedral Pt-Ni/C NPs:**

The NP in Figure 1 and Figure 2 is the same NP on a MEMS chip. The NP in Figure S 2 is on the same MEMS chip as the NP in Figure 1 and Figure 2.

**Irregular Ni-rich Pt-Ni/C reference nanoparticles:**

The NPs in Figure S 5 A-E and F-J are the same NP on a MEMS Chip.

**Pt-Ni reference nanoparticles without C:**

The NPs in Figure S 6 A-D and E-H are the same NPs on a MEMS chip.

***In situ* TEM measurements under oxidizing conditions.** The C-supported Pt-Ni octahedral nanoparticles were dispersed on a MEMS chip (DENSsolutions B.V.). The chip was loaded into a gas reaction heating holder (DENSsolutions B.V.) and examined in 1.1 bar of O<sub>2</sub> in the nanoreactor.

**Core-shell octahedral Pt-Ni/C NPs:**

The NPs in Figure 3, Figure 4, Figure S 3 and Figure S 7 are the same NPs on a MEMS chip.

**Thermal gravimetric analysis (TGA) coupled to a mass spectrometer (MS).** TGA was conducted on an STA 449 F5 Jupiter® from Netsch (Selb, Germany), which was interfaced to an MS via a heated gas transfer system in an oxygen atmosphere, with heating performed from room temperature to 500 °C. MS readings were recorded using a QMS 403 D Aëolos® quadrupole mass spectrometer from Netzsch (Selb, Germany). The mass range of the spectrometer unit is between 1-300 atomic mass units (amu). Ionization of the sample gas was carried out at 70 eV, with the pressure set to 1 bar during the experiment.

**Morphological, structural, and elemental characterization**

Surface atomic arrangements were observed by high-resolution TEM (HRTEM) on an Thermo Scientific™ Titan 80-300 electron microscope<sup>3</sup> equipped with a spherical aberration (C<sub>s</sub>) corrector (CEOS) for the objective lens. Experiments were carried out at 300 kV using the negative-C<sub>s</sub> imaging technique, which provides images with high contrast and low noise. Scanning TEM (STEM) and energy dispersive X-ray spectroscopy (EDX) experiments were performed in an Thermo Scientific™ Titan 80-300 electron microscope equipped with a probe corrector (CEOS) and an High angle annular dark field

(HAADF) detector<sup>4</sup>. “Z-contrast” conditions were achieved by using a probe semi-angle of 25 mrad and an inner collection angle of the detector of 68 mrad.

### Additional information

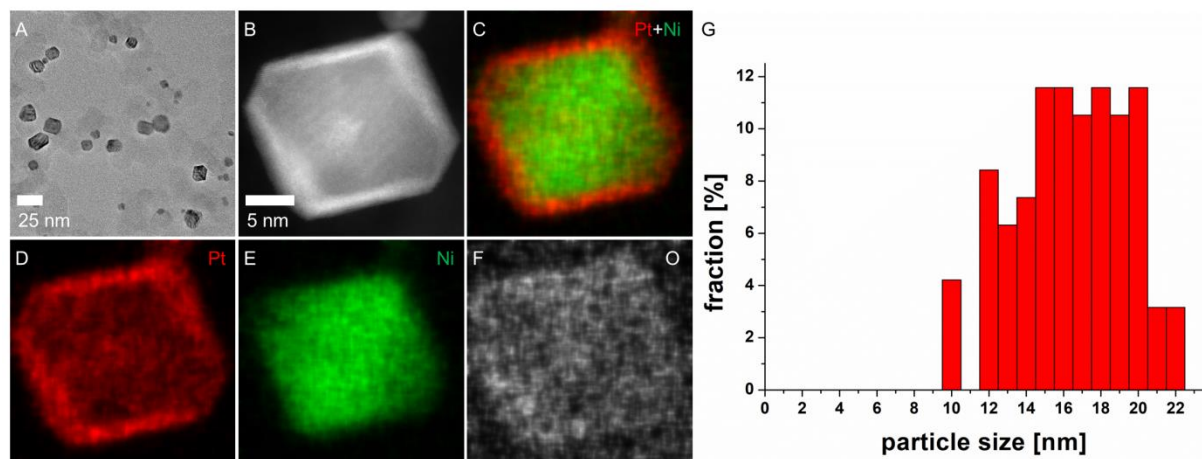


**Figure S 1: Bright field TEM image, HAADF STEM image and EDX composition maps of C-supported Pt-Ni octahedral NPs. (A) Overview TEM image of the particles; (B) High resolution STEM image; (C-F) Pt (red), Ni (green) and O (white) EDX composition maps of a NP in its initial state; (G) Size distribution for Pt-Ni octahedral nanoparticles.**

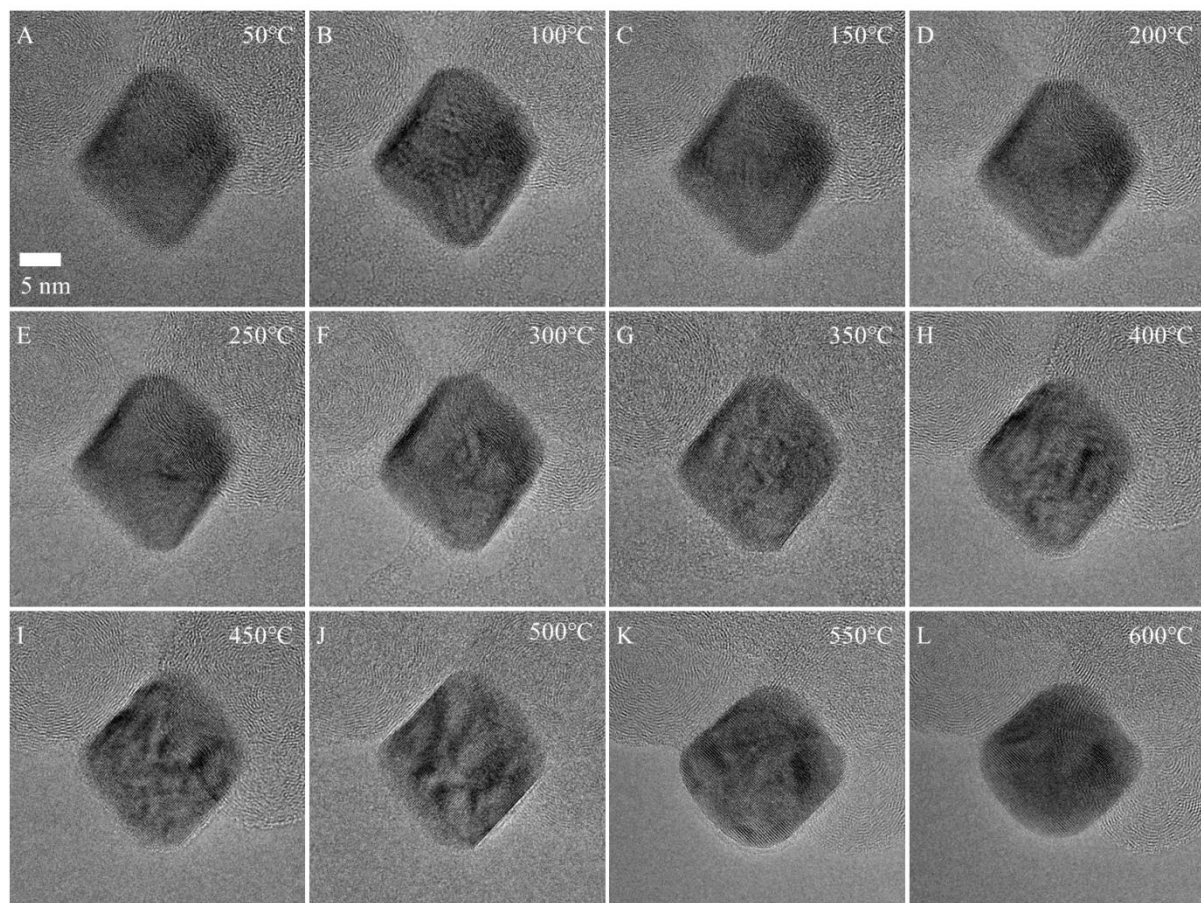


**Figure S 2:** (A-L) HRTEM images of Pt-Ni octahedral NPs recorded during *in situ* thermal annealing between 50 and 600 °C.

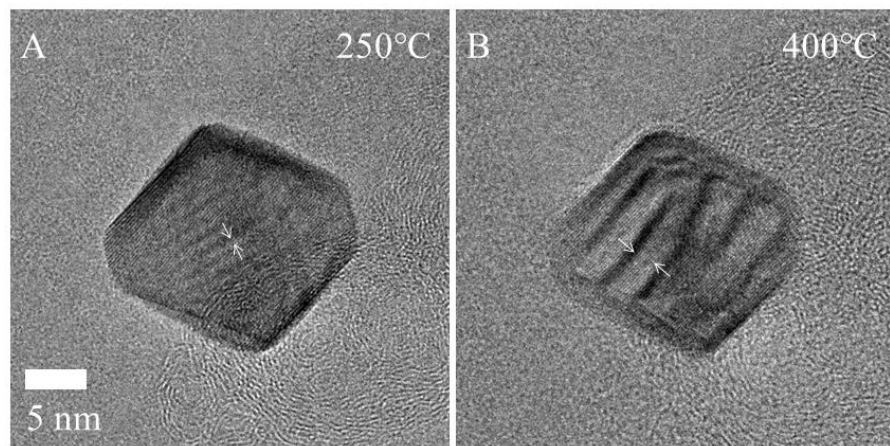


**Figure S 3:** (A-B) Bright-field TEM images of an octahedral NP recorded at (A) 250 °C and (B) 400 °C in vacuum. The arrows in (A) and (B) mark Moiré fringe spacing of 0.49 nm and 2.07 nm, respectively. Further details are provided in the text.

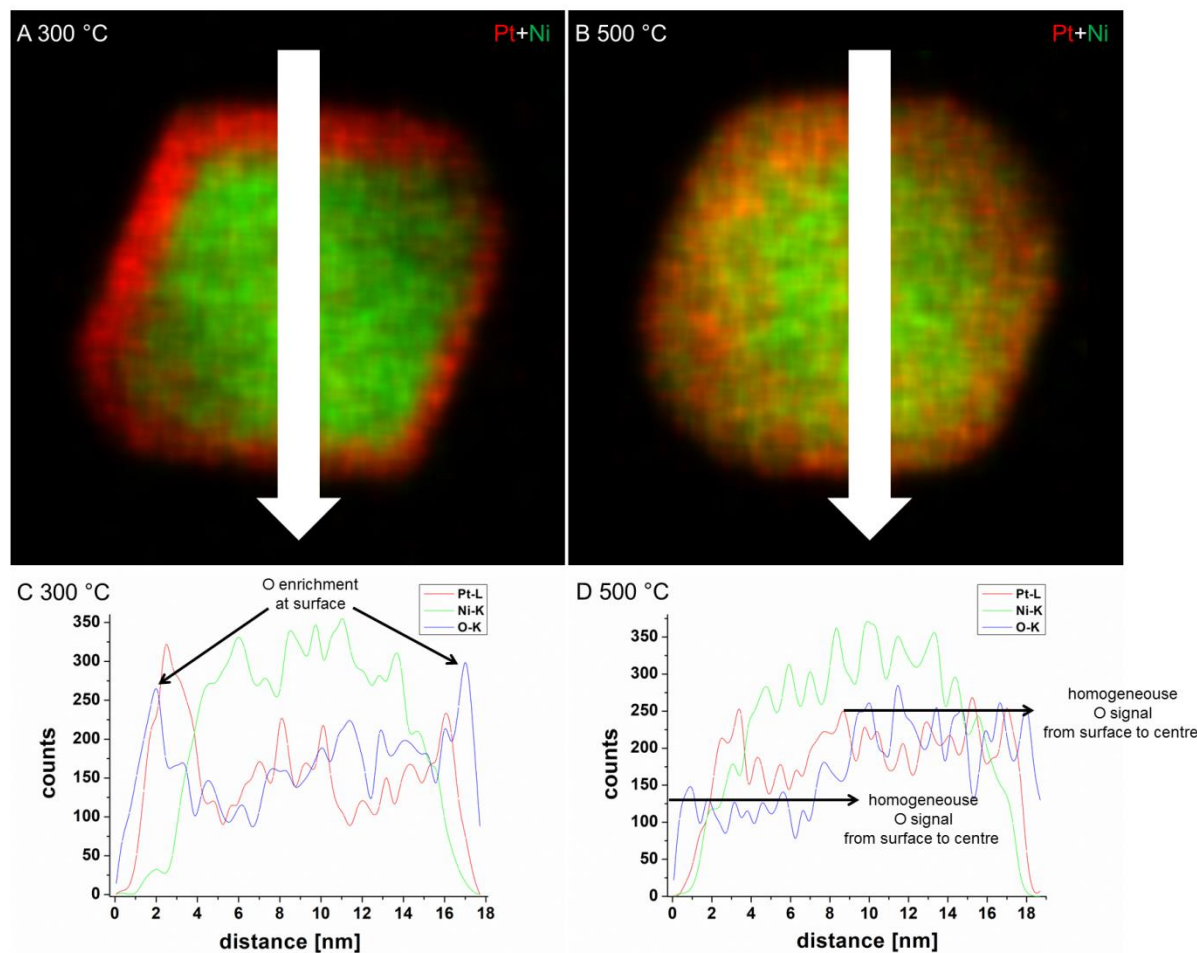


**Figure S 4: EDX elemental maps and line scans showing the compositions of octahedral Pt-Ni core-shell NPs after annealing at (A, C) 300 °C and (B, D) 500 °C. Pt (red), Ni (green) and O (blue) signals are shown in the EDX maps and line scans. Arrows in (A) and (B) show the directions of the line scans.**

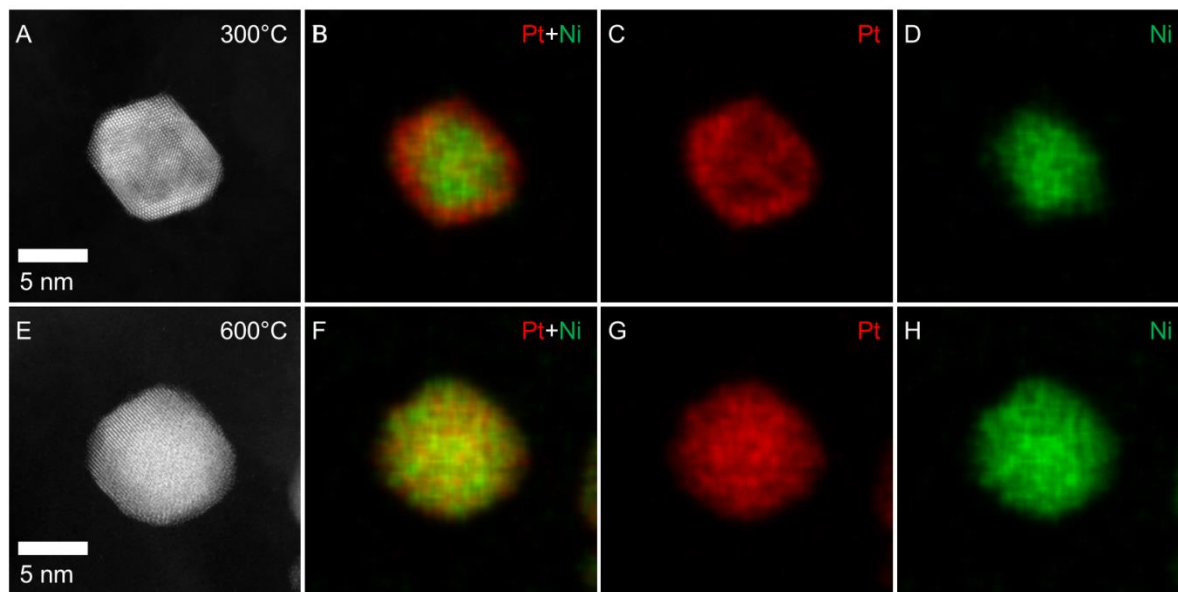


**Figure S 5: HAADF STEM images and EDX composition maps of a Pt-Ni octahedral nanoparticle. (A, E) High-resolution HAADF STEM images of a nanoparticle oriented close to  $\langle 110 \rangle$  after annealing at (A) 300 °C and (E) 600 °C. (B-D) and (F-H) show corresponding Pt (red) and Ni (green) signals in qualitative EDX composition maps.**

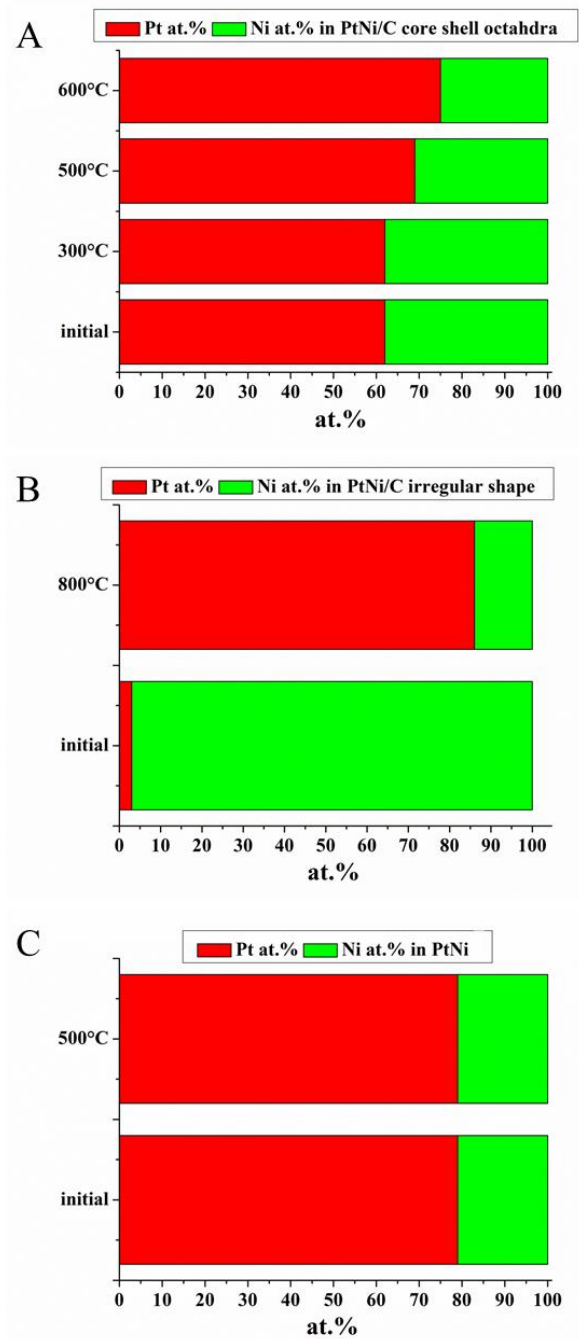
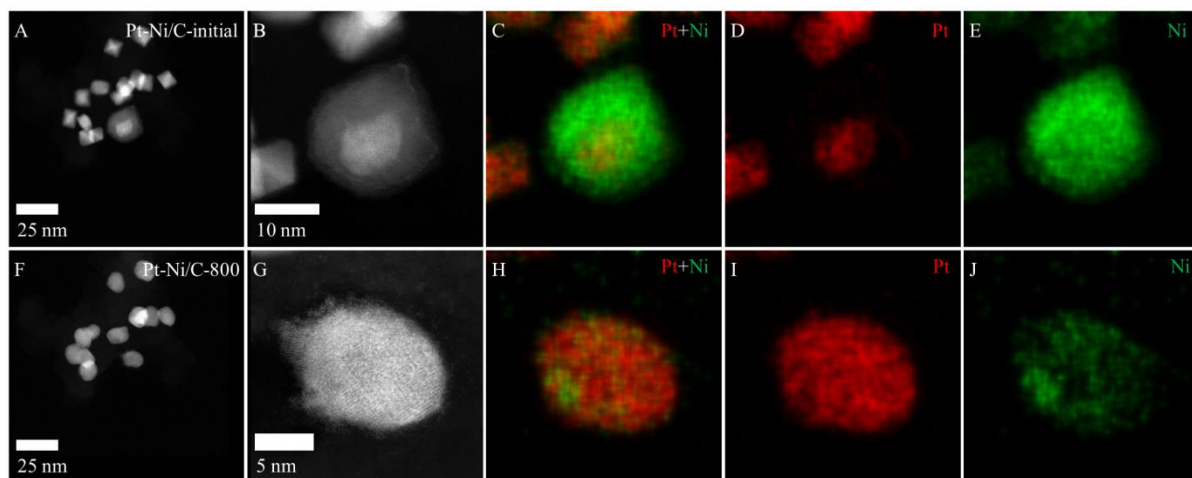
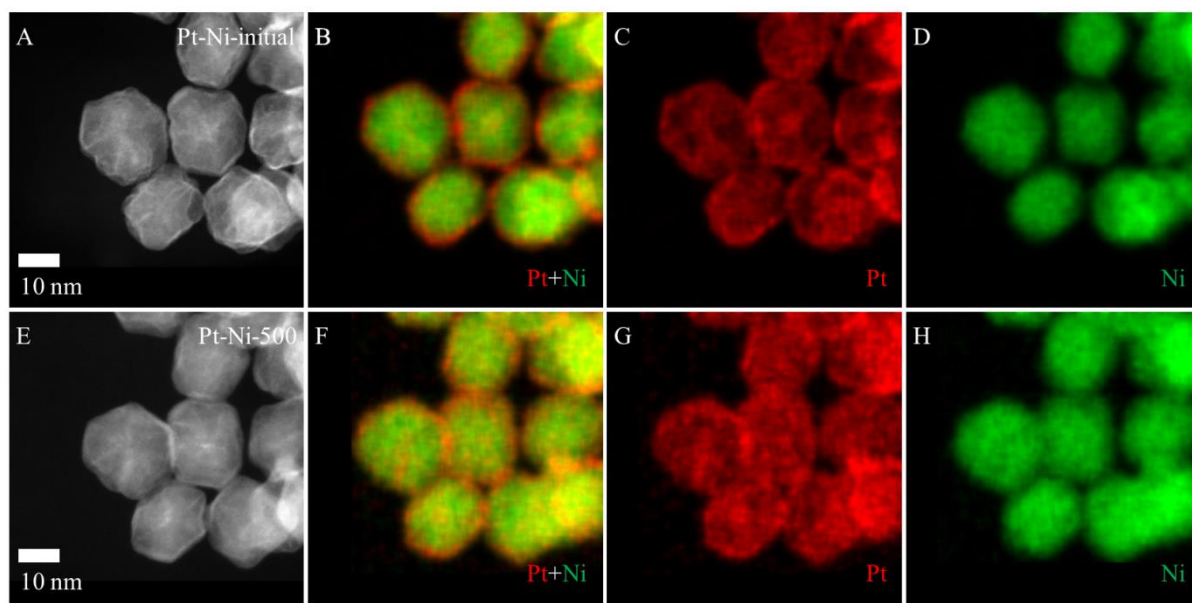


Figure S 6: (A-C) Diagrams for the average composition of the C supported PtNi octahedral core shell particles (A), the C supported Pt-Ni irregular shaped NPs (B) and the Pt-Ni NPs (C).





**Figure S 7: HAADF STEM images and EDX elemental maps of C-supported irregular Ni-rich Pt-Ni nanoparticles. (A, F) HAADF STEM overview images of the Pt-Ni nanoparticles in their (A) initial and (F) annealed (800 °C) state. (B, G) High-resolution HAADF STEM images of Pt-Ni nanoparticles in their (B) initial and (G) annealed (800 °C) state. (C-E) and (H-J) Pt (red) and Ni (green) in EDX composition maps of the corresponding nanoparticles.**



**Figure S 8: HAADF STEM images and EDX elemental maps of Pt-Ni nanoparticles. (A, E) HAADF STEM images of the Pt-Ni nanoparticles in (A) their initial state and (E) after annealing reducing condition at 500 °C. (B-D) and (F-H) Pt (red) and Ni (green) in EDX composition maps of the corresponding nanoparticles.**

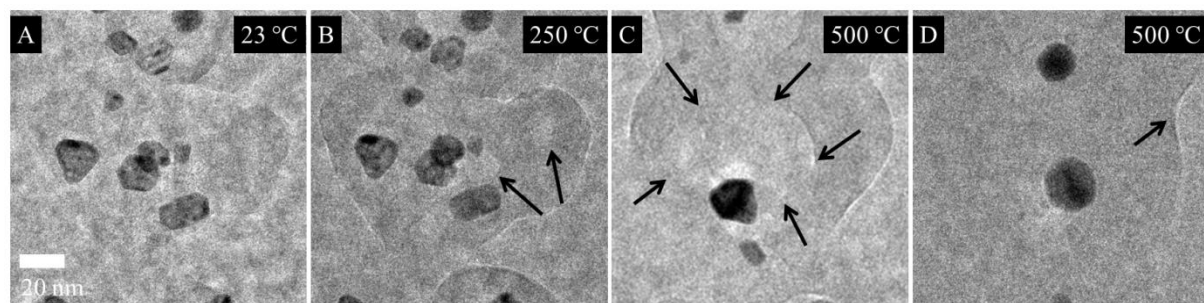


**Figure S 9:** (A-D) Bright-field TEM images recorded at (A) 23 °C, (B) 250 °C, (C and D) 500 °C in 1.1 bar of oxygen showing changes to the C support. Arrows in (B) and (C) mark the formation of a discontinuous C structure in the C support. The arrow in (D) marks the remaining amorphous C layer. Further details are provided in the text.

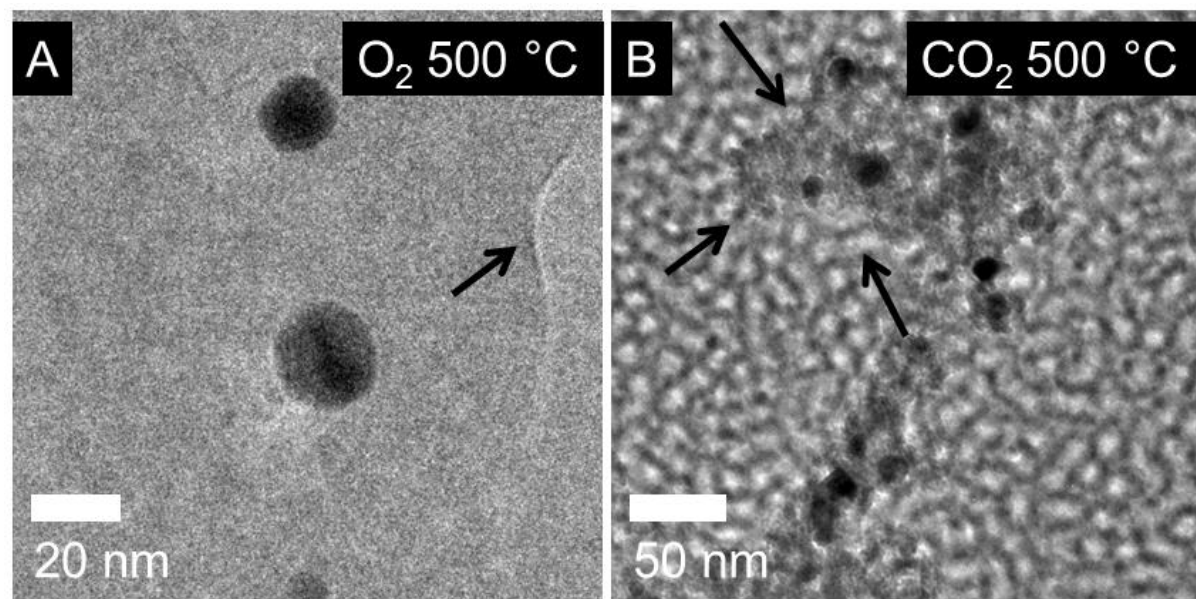


**Figure S 10:** (A, B) Bright-field TEM images recorded at (A) 500 °C in 1.1 bar of O<sub>2</sub> and (B) 500 °C in 1.1 bar of CO<sub>2</sub>, showing different changes to the C support. Arrows in (A) and (B) mark the remaining C structures in the C support. Further details are provided in the text.

## Reference

- 1 V. Beermann, M. Gocyla, S. Kühl, E. Padgett, H. Schmies, M. Goerlin, N. Erini, M. Shviro, M. Heggen, R. E. Dunin-Borkowski, D. A. Muller and P. Strasser, *J. Am. Chem. Soc.*, 2017, **139**, 16536–16547.
- 2 M. Shviro, S. Polani and D. Zitoun, *Nanoscale*, 2015, **7**, 13521–13529.
- 3 A. Thust, J. Barthel and K. Tillmann, *J. large scale Res. Facil.*, 2016, **2**, A41.
- 4 A. Kovács, R. Schierholz and K. Tillmann, *J. large scale Res. Facil.*, 2016, **2**, A43.